Received: 24 September 2021 | Accepted: 17 January 2022

DOI: 10.1111/bpa.13054

Brain Pathology

RESEARCH ARTICLE

The association between neurodegeneration and local complement activation in the thalamus to progressive multiple sclerosis outcome

Benjamin J. Cooze[1] | **Matthew Dickerson**[1] | **Rukshikah Loganathan**[1] | **Lewis M. Watkins**[1] | **Ethan Grounds**[1] | **Ben R. Pearson**[1] | **Ryan Jack Bevan**[2] | **B. Paul Morgan**[2] | **Roberta Magliozzi**[3] | **Richard Reynolds**[4] | **James W. Neal**[1] | **Owain W. Howell**[1]

[1]Faculty of Medical, Health and Life Sciences, Swansea University, Swansea, UK

[2]UK Dementia Research Institute at Cardiff University, Cardiff, UK

[3]Department of Neurological and Movement Sciences, University of Verona, Italy

[4]Division of Brain Sciences, Imperial College London, London, UK

Correspondence
Owain W. Howell, Institute for Life Sciences, Faculty of Medical, Health and Life Sciences, Swansea University, Singleton Park Campus, Swansea SA2 8PP, UK.
Email: o.w.howell@swansea.ac.uk

Funding information
This work was supported by grant funding from the UK MS Society (993), Life Science Research Network Wales and Swansea University (SURES award).

Abstract

The extent of grey matter demyelination and neurodegeneration in the progressive multiple sclerosis (PMS) brains at post-mortem associates with more severe disease. Regional tissue atrophy, especially affecting the cortical and deep grey matter, including the thalamus, is prognostic for poor outcomes. Microglial and complement activation are important in the pathogenesis and contribute to damaging processes that underlie tissue atrophy in PMS. We investigated the extent of pathology and innate immune activation in the thalamus in comparison to cortical grey and white matter in blocks from 21 cases of PMS and 10 matched controls. Using a digital pathology workflow, we show that the thalamus is invariably affected by demyelination and had a far higher proportion of active inflammatory lesions than forebrain cortical tissue blocks from the same cases. Lesions were larger and more frequent in the medial nuclei near the ventricular margin, whilst neuronal loss was greatest in the lateral thalamic nuclei. The extent of thalamic neuron loss was not associated with thalamic demyelination but correlated with the burden of white matter pathology in other forebrain areas (Spearman $r = 0.79$, $p < 0.0001$). Only thalamic neuronal loss, and not that seen in other forebrain cortical areas, correlated with disease duration (Spearman $r = -0.58$, $p = 0.009$) and age of death (Spearman $r = -0.47$, $p = 0.045$). Immunoreactivity for the complement pattern recognition molecule C1q, and products of complement activation (C4d, Bb and C3b) were elevated in thalamic lesions with an active inflammatory pathology. Complement regulatory protein, C1 inhibitor, was unchanged in expression. We conclude that active inflammatory demyelination, neuronal loss and local complement synthesis and activation in the thalamus, are important to the pathological and clinical disease outcomes of PMS.

KEYWORDS
atrophy, complement activation, CSF, meningeal inflammation, microglial activation, neuron loss

1 | INTRODUCTION

Widespread demyelination, inflammation and neurodegeneration are characteristics of progressive multiple sclerosis (PMS) [1]. Regional tissue volume loss, be it in the cortical grey, white or deep grey matter, reflects the extent of myelin and neuronal pathology, and is an important surrogate measure of disease outcome [2-5]. Magnetic resonance imaging has demonstrated that an increased number of lesions in the deep grey matter are predictive of disease course and thalamic atrophy is an early imaging feature of MS [6-8]. A disease-specific reduction in thalamic volume begins early and progresses steadily, regardless of the MS subtype [9]. Much recent interest has focussed on how deep grey matter and thalamic atrophy may predict later clinical outcomes [5–12].

The deep grey matter nuclei, including the basal ganglia and thalamus, are particularly affected in PMS. Demyelination, inflammation, and neuronal loss can be substantial and the extent and pattern of this pathology relate spatially to the CSF-ependymal barriers as well as to distal pathology in the adjacent white matter, through processes of antero/retrograde degeneration [13-17]. Both vascular and CSF-meningeal effectors of demyelination and neurodegeneration abound in later diseases [18-21]. Inflammatory chemokines, cytokines, mediators of oxidative injury, blood-derived serum proteins, including fibrin and complement proteins, which can be generated locally as well as systemically, are elevated and have been shown to effect disease-relevant pathological processes associated with a more severe clinical outcome [22-24].

Activated complement is a component of central inflammation in MS, both in the early and later, progressive phase [25-27]. Synaptic and neuritic degeneration is one underlying cause of tissue volume loss and synaptic pruning is driven by complement C3 mediated opsonisation and uptake by complement receptor-bearing microglia [28]. Complement proteins are elevated in early and chronic MS [29-33] and in the brain are localised to sites of ongoing inflammatory demyelination [27,34–40]. Genome-wide association studies demonstrate that complement C3 gene variants predispose some people with MS to accelerated retinal neuropathology [41]. Whilst patients with a greater number of chronic active lesions harbour more risk variants in early complement genes, including C1q and C3 [40]. C1q and products of C3 are present in the MS retina, hippocampus and thalamus, where they represent a modifiable target in experimental models, supporting a role for products of early complement activation, up to and including C3, in disease pathogenesis [40,42–44]. Together with a chronic over-activation of complement, complement regulation, a crucial check-point to prevent damaging complement release or to accelerate the breakdown of activated complement, maybe dysfunctional in MS and other neurodegenerative diseases [33,38,45–49].

We hypothesised that the extent of thalamic damage is an important correlate of clinical disease severity, and that neuron loss and local complement activation are important to this process. To address our hypothesis, we quantified the extent of thalamic demyelination, neurodegeneration and complement activation in samples of thalamus and neocortex, from PMS and age and region-matched controls.

2 | MATERIALS AND METHODS

2.1 | Cohorts and sampling strategy

Tissue from 21 progressive MS (17 secondary progressive MS and 4 primary progressive MS [PPMS]), 10 non-neurological control cases, 4 inflammatory disease controls (viral encephalitis) and three cases of ischaemic encephalopathy were provided by the MS Society Tissue Bank and the Oxford Brain Bank (under research ethical approval 13/WA/0292 and 08/MRE09/31). Cases were pooled as the pathological mechanisms and overall burden of tissue damage underlying PP and SPMS are broadly similar [50,51]. Sampled areas, neuroanatomically matched between cases and irrespective of the presence or absence of macroscopically visible lesions, were selected by the attendant neuropathologist and included the frontal cortex, cingulate cortex, thalamus and the hippocampus/temporal lobe (please see Table 1 and Figure 1 for details). All blocks, with the exception of those used for *in situ* hybridisation, were formalin-fixed and paraffin-embedded as standard and sectioned at 6 μm.

2.2 | Identification of thalamic nuclei and extra thalamic structures

The thalamus was sub-divided into medial and lateral nuclei groups according to the anatomical and cytoarchitectonic descriptions of Macchi and Jones [52] and with reference to the Allen Brain atlas [53]. The intralaminar nuclear complex (central lateral nucleus, centromedian, paracentral and paracentral nuclei) served as the boundary between medial and lateral nuclear groups. The medial thalamic group of nuclei contained the periventricular medial dorsal and anterior thalamic nuclei, both easily identifiable and adjacent to the ventricular lumen. The anterior and posterior groups of the intralaminar nuclear complex were considered part of the lateral thalamic complex of nuclei, alongside the ventrolateral nucleus, extending laterally to the boundary with the internal capsule. The zona incerta was used as the boundary marker to differentiate the thalamus from sub-thalamic nuclei.

TABLE 1 Details of multiple sclerosis, non-neurological and other neuroinflammatory disease (ONID) controls used in this study

Multiple sclerosis	Disease	Gender	Disease duration	Age at death	Cause of death	Available blocks
MS402	SPMS	M	20	46	MS, bronchopneumonia	4
MS405	SPMS	M	25	62	MS, septicaemia, metastatic colon cancer	4
MS407	SPMS	F	19	44	Septicaemia, pneumonia	4
MS408	SPMS	M	10	39	Pneumonia, septicaemia	4
MS422	SPMS	M		58	Chest infection because of MS	4
MS423	SPMS	F	30	54	Pneumonia	4
MS425	SPMS	F	21	46	MS, pneumonia	4
MS438	SPMS	F	18	53	MS	4
MS444	SPMS	M	20	49	Renal failure	4
MS473	PPMS	F	13	39	MS, pneumonia	4
MS485	PPMS	F	29	57	MS, pneumonia	4
MS491	SPMS	F	26	64	Anaphylactic reaction	4
MS492	PPMS	F	31	66	Sigmoid cancer	4
MS497	SPMS	F	29	60	MS, pneumonia	4
MS510	SPMS	F	22	38	MS, pneumonia	4
MS513	SPMS	M	18	51	MS, respiratory failure	4
MS517	PPMS	F	25	48	MS, septicaemia	4
MS527	SPMS	M	25	47	MS, pneumonia	4
MS528	SPMS	F	25	45	MS	4
MS530	SPMS	M	24	42	MS	4
MS538	SPMS	F	39	62	MS, pneumonia	4
N = 21	17 SPMS 4 PPMS	13 F 8 M	24.5 year (10–39)	49 year (38–66)		

Controls	Gender	Age at Death, year	Cause of death	Available blocks
CO25	M	35	Carcinoma of the tongue	4
12/023	M	69	Unknown	4
12/046	M	72	Unknown	4
12/048	F	55	Ovarian cancer	4
12/052	F	42	Pancreatic cancer	4
12/088	M	51	Coronary heart disease	4
11/093	F	52	Chronic liver disease	4
11/122	F	65	Chronic obstructive pulmonary disease	4
12/132	F	67	Unknown	4
1231/93	M	58	Unknown	4
N = 10	5 F 5 M	56 year (35–72)		

ONID controls	Disease	Gender	Disease duration	Age at death, year	Cause of death	Available blocks
B 4938	HSV encephalopathy	M	n/d	18	N/A	4
C2342	HIV encephalopathy	M	n/d	17	Brain stem granuloma	4
C3727	HIV encephalopathy	M	n/d	41	Encephalopathy and myelopathy	4
C4178	CMV encephalopathy	M	n/d	59	Encephalopathy	4
1062/00	Ischaemic encephalopathy	F	n/d	49	Unknown	1

(Continues)

TABLE 1 (Continued)

ONID controls	Disease	Gender	Disease duration	Age at death, year	Cause of death	Available blocks
1078/95	acute and severe ischaemic encephalopathy	M	n/d	32	Ischaemic encephalopathy	1
1140/95	Ischaemic encephalopathy	F	n/d	10	Ischaemic encephalopathy	1

Note: The median age of death and disease duration are shown in years where applicable (with range). Available blocks indicate the number of unique brain tissue blocks analysed per case - corresponding to superior frontal gyrus, cingulate gyrus, inferior temporal lobe and thalamus.

Abbreviations: F, female; M, male; n/a, not applicable; n/d, not determined; PP, primary progressive; SP, secondary progressive.

TABLE 2 Primary antibodies used in this study. Antibody name, target, clonality and source

Antigen	Clone and source	Dilution	Product code
Myelin oligodendrocyte glycoprotein	Ms mc (Z12) In house	1:50	–
Proteolipid protein	Ms mc (PLPC1) AbD serotec/Merck	1: 2000	MCA839G
Human Leukocyte Antigens DP-DQ-DR	Ms mc (cr3/43) Dako/Agilent	1: 200	M0775
ionised calcium binding adapter molecule1	Polyclonal Wako/Fuijifilm	1: 1000	019-19741
Human HuC, HuD & Hel-N1 neuronal proteins	Ms mc (16A11) Fisher	1: 1500	11524027
Glial fibrillary acidic protein	Polyclonal Dako/Agilent	1: 1200	Z0334
Complement pattern recognition protein C1q	Polyclonal Dako/Agilent	1: 800	A013602-2
Complement activation fragment C4d	Ms mc Pathway Diagnostics	1: 400	A213
Complement activation fragment Bb	Ms mc Pathway Diagnostics	1: 400	A252
Complement activation fragments C3b and iC3b	Ms mc (C3-30) In house	1: 500	–
Complement C9 neo antigen (MAC)	Ms mc (B7) In house	1: 200	–
Complement C1inhibitor	Polyclonal In house	1: 500	–

Note: Epitope retrieval was performed in 0.05% citraconic anhydride (v/v).

Abbreviation: Ms mc, mouse monoclonal antibody.

2.3 | Single and dual-labelling immunohistochemistry

All single and dual-label tissue staining was carried out using standard avidin-biotin amplification with either a peroxidase or phosphatase enzyme-linked detection system and diaminobenzidine or vector blue (Vector labs) as the chromogen [32]. Immunohistochemistry-identified essential components of myelin, monocytes (overwhelmingly activated microglia/macrophages in the brain parenchyma), post-mitotic neurons and components of the complement system (all primary antibodies used in this study are listed in Table 2). All sections from all cases were immunostained for a single or dual target as part of the same experiment and included primary antibody-negative controls and irrelevant species-specific antisera as positive controls.

2.4 | Digital pathology workflow

Whole stained sections for control and PMS were digitised using a ZEISS Axio Scanner and the resulting annotated.czi files managed as a project within QuPath (https://qupath.github.io/; [54]). Gross anatomy was first delineated using the scanned LFB-stained section of each case to outline the area of cortical and sub-cortical white matter (cortical blocks) and thalamic nuclei (medial and lateral nuclei). Following the outlining of anatomical ROIs, and using the QuPath multi-image viewer, annotations generated from the LFB section were then overlaid onto the subsequent anti-MOG and anti-HLA-D slides, so that areas of demyelination and lesion inflammatory activity could be calculated with reference to tissue architecture. Lesion and non-lesion annotations per anatomical ROI were then transferred to the sequential

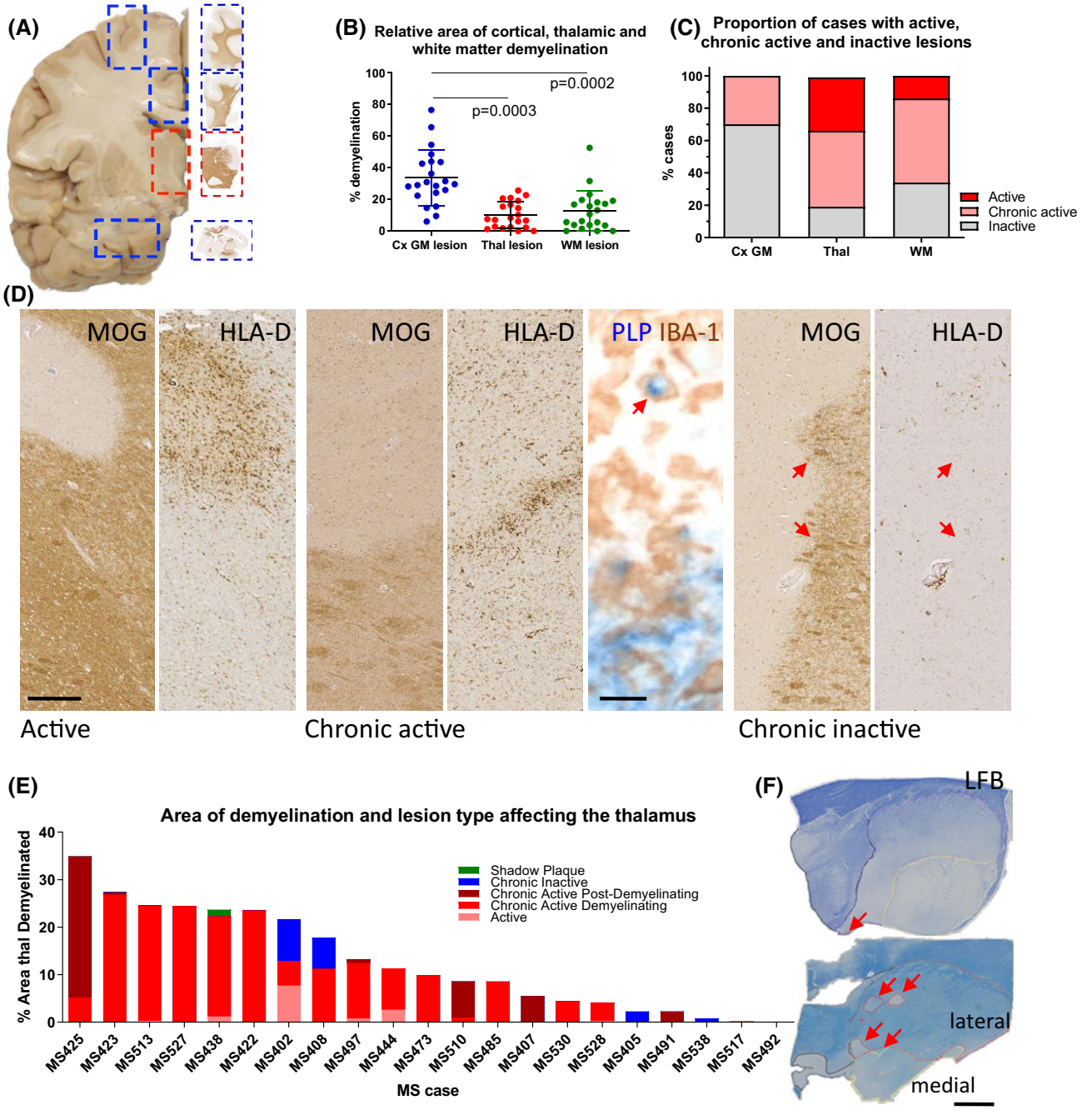

FIGURE 1 Inflammatory demyelination in cortical, white matter and thalamus of progressive MS. (A) Neuroanatomical matched blocks of frontal gyrus, cingulate gyrus, thalamus and temporal lobe (inferior) were sampled to quantify the number and extent of demyelinating lesions per case. (B) Samples of cortical grey matter (Cx GM lesion) displayed the greatest and most varied extent of demyelination as a proportion of total measured cortical grey matter, compared to that seen in paired thalamus (thal lesion) and sub-cortical white matter (WM lesion) areas. (C) Characterisation of lesions based on their inflammatory activity revealed the thalamus had a greater proportion of cases displaying inflammatory active and chronic active demyelinating lesions than cortical grey or white matter. (D, E) The relative area occupied by active, chronic active (demyelinating or post-demyelinating; note the presence of PLP+ material within an IBA-1+ macrophage, arrow), inactive or fully remyelinated (shadow plaque) lesions plotted per thalamus per case in descending order (% area thal demyelinated). Note the majority of cases were characterised by an overtly active/chronic active thalamic demyelinating pathology with n = 4/21 presenting only inactive lesions. (F) Representative example from a case displaying <0.1% demyelination of total thalamus area (MS492, red arrow) and a case presenting with 24.4% of total thalamus affected by active demyelination (MS438, red arrows). Friedman's paired test with Dunn's multiple comparison post-test. Scale bars: D = 100 μm (except PLP, IBA-1 image = 10 μm); F = 5 mm

anti-HuC/D and anti-complement immunostained slides to guide the automated quantification of these markers.

2.5 | Lesion classification

Inflammatory demyelinating lesions of the thalamus and cortical white and grey matter were categorised dependent on the density and distribution of HLA-D+ microglia/macrophages. Active (A), chronic active demyelinating (CAD) or chronic active post-demyelinating (CAPD) lesions were differentiated based on the presence/absence of recently phagocytosed myelin protein (PLP+) within phagocytes (IBA-1+; revealed by dual colour immunohistochemistry according to published criteria [55]). Chronic Inactive (CI) demyelinating lesions presented a well-demarcated lesion edge with few reactive microglia-like cells. Cortical grey matter lesions were characterised based on their location within the cerebral cortex [55].

2.6 | Quantification of neurons

Automated cell counting of anti-HuC/D+ neurons was performed in QuPath by first estimating stain vectors (to first optimise the automatic detection of brown DAB reaction product through a process of colour deconvolution and optimisation of parameters to define the background and immuno-positive signal). Using the positive cell detection command, we then determined the total number of anti-HuC/D+ neurons (defined as being >60 μm^2 to discount any immunoreactive oligodendrocyte-like cells) in the total lesion and normal-appearing tissue of the medial and lateral thalamus, respectively. Our optimised counting command was compared to manual counting across 110 ROIs from 8 representative cases where there was a > 97% agreement between manual and automated counts (data not shown). Anti-HuC/D+ neuron counts were determined per individual lesion per thalamic ROI and later combined to give the mean HuC/D+ cell density in medial and lateral lesions, respectively. All neurons in the normal-appearing thalamus were counted. Control anti-HuC/D cell counts were captured from the entire medial and lateral nuclei, respectively.

2.7 | Quantification of complement recognition molecules, activation fragments, regulator proteins and the extent of microglial/macrophage activation

C1q, the recognition molecule of the classical pathway, was used to demonstrate classical pathway engagement, whilst the presence of C4d, an activation product of C4, revealed early classical pathway activation. Complement activation fragments C3b and iC3b demonstrate cleavage of C3, the convergence point of all the complement pathways. Complement activation fragment Bb demonstrates cleavage of factor B, a marker of alternative complement pathway activation, whilst C1-inhibitor (serping1), a regulator of the C1 activation complex, was examined to investigate classical pathway regulation. The presence of the cytolytic membrane attack complex (MAC, C5b-9) was detected using an anti-C9neo antibody. The positive pixel count command was used to determine the per cent area of anti-complement immunoreactivity (as complement immunoreactivity represented both cell and neuropil-associated signal) and the area of immunoreactivity in lesion, non-lesion and control thalamic ROIs captured. Measurements were taken from both lesion centre and lesion edge per lesion class (active, CAD and CI lesions) and from areas of normal thalamus (defined as being >10 mm away from the nearest area of inflammatory demyelination), per case with available lesion types of interest. The area of anti-HLA-D+ immunoreactivity was captured from the same equivalent normal-appearing thalamus ROIs used to capture the complement data.

2.8 | In situ hybridisation

To detect single mRNA molecules of complement *C1QA* (Homo sapiens C1q A chain, NM_001347465.2) and *C3* (Homo sapiens complement *C3*, NM_000064.4), we used BaseScope triple-z probes (Advanced Cell Diagnostics, Bio-techne Ltd). Probe detection was performed on 10 μm thick frozen sections prepared from 2 control (12/048 and 12/052) and 4 PMS cases (MS422, MS425, MS527 and MS538), alongside positive (Homo sapiens *PPIB*), negative (*Escherichia coli DAPB*) and no-probe (blank) control slides. Sections were thawed, immediately fixed, washed and dehydrated, before treating with H_2O_2 prior to antigen retrieval and probe incubation (2 h at 40°C using the ACD HybEZ system). Specific probe binding was detected using the BaseScope Detection Reagent Kit v2 according to the manufacturer's instructions, using fast red as the chromogen. Sections were then processed for subsequent anti-HuC/D immunohistochemistry following washing in Tris-HCl buffer, peroxidase and phosphatase quenching using Bloxall endogenous blocking solution (Vector Labs, Inc.) and overnight incubation with primary antibody for Avidin-Biotin and alkaline phosphatase and vector blue chromogenic detection, as described above. Sections were mounted in Vectamount (Vector Labs, Inc.) and viewed with a Zeiss Axio Scope 1 at 100-630x magnification fitted with a Zeiss MRm 503 colour camera. Positive control probe *PPIB* yielded widespread cell-specific signal as anticipated, whilst *DAPB* and blanks were negative (images not shown).

2.9 | Statistical analysis

Statistical analysis and graphing were performed using GraphPad Prism (v. 9.1.1). The majority of data were non-normally distributed (Shapiro-Wilks test for normality) and non-parametric statistical analysis methods were applied throughout. Data was presented on a per-case basis in scatter plots with group mean and standard deviations (SD) displayed. Differences between two groups (for example, the relative extent of demyelination of medial versus lateral thalamic samples) was compared using the unpaired Mann–Whitney test. When comparing three or more groups (e.g. when comparing HuC/D+ neuron density in control, non-lesion and lesion medial or lateral thalamic samples) the Kruskal–Wallis test with Dunn's multiple comparison post-test was used. Spearman correlation was used to test for statistically significant associations between groups (e.g. between the relative extent of neuron loss in the non-lesion MS thalamus to the reported age of death or duration of disease) and the Spearman *r*- and *p*-values reported in each instance. Statistical significance was considered when $p < 0.05$.

3 | RESULTS

We conducted an analysis of lesions, microglial and complement activation, and neuronal loss, in samples of the thalamus and paired cortical blocks to assess the pathological burden, and the immune mechanisms, associated with progressive MS disease outcome.

3.1 | Demyelination in cortical and thalamic blocks

We first quantified the area of thalamic, cortical grey matter and sub-cortical white matter demyelinated lesions in 21 PMS cases (Figure 1A). The mean per cent lesion area of cortical grey matter demyelination in samples of the frontal, cingulate and temporal cortex was greater than the extent of demyelination of the thalamus (total thalamus) or sub-cortical white matter (total white matter in the same frontal, cingulate and temporal lobe blocks; Figure 1B). Percentage area of demyelination varied from 6.0% to 76.5% (mean = 33.7%) for cortical grey matter, 0%–52.6% (mean = 12.8%) for sub-cortical white matter and 0.1%–25.6% (mean = 10.09%) for the thalamus.

3.2 | Active inflammatory demyelinating lesions of the thalamus are more common than in other brain areas

We annotated and quantified the number and area of individual demyelinated lesions, classified based on microglia/macrophage density and evidence of recent demyelinating activity (Figure 1C,D). By comparing the incidence and relative size of thalamic lesions to lesions of the cortical grey and white matter, we found that the proportion of cases containing active and chronic active and demyelinating (CAD) lesions in the thalamus was greater than the number of cases displaying active or CAD grey or white matter lesions in the cortical blocks (Figure 1C). The area occupied by active and CAD thalamic lesions (13.4 ± 30% and 73.4 ± 40%, respectively) was greater as a proportion of the total lesion area than it was for cortical active (0%) and CAD (5.8 ± 12%) lesions in the same case ($p < 0.05$). The proportion of thalamic lesions of each class was similar to that seen in the sub-cortical white matter (9.4 ± 23% classified as active, 53.8 ± 44% classified as CAD; Figure 1C,D). By plotting the relative proportion of each type of lesion per case, we show how affected the PMS thalamus was by active and chronic active and demyelinating lesions (Figure 1E,F).

3.3 | Demyelination was more extensive in the medial thalamic nuclei

The distribution of the individual lesions was assessed in the medial nuclei adjacent to the ependymal lining of the 3rd ventricle and the more lateral thalamic nuclei (Figure 2). The extent of demyelination was greater in the medial thalamic nuclei compared to the lateral thalamic nuclei (Figure 2A). Individual thalamic lesions of the medial nuclei were typically larger (Figure 2B) and were mainly classified as periventricular (i.e. lying directly adjacent to and associated with the ependyma). The number of perivascular lesions (all other lesions) was greater, but they were smaller in area, in comparison to those classified as periventricular. The overwhelming majority of both periventricular and perivascular lesions were classified as active or CAD (Figure 2B,C).

3.4 | Neurodegeneration and microglial activation were present throughout the thalamus

Neuron densities (Figure 3A) were reduced in the lesion and non-lesion medial and lateral thalamic nuclei, compared to controls. Neuronal loss was variable (0–68.9% reduction compared to control), with a mean of 16.6% reduction in the non-lesion and 38.8% reduction for the lesion medial nucleus, and a 28.3% and 45.1% reduction in the non-lesion and lesion lateral nuclei, respectively (Figure 3B). The per cent reduction in neuron count was greater for the lateral non-lesioned nuclei in comparison to the medial nuclei ($p = 0.039$, Wilcoxon paired test), but the extent of neuron loss between medial and lateral lesions was not different ($p = 0.153$).

The reduction in thalamic neuron density was equal to or substantially greater than that seen in the cortical

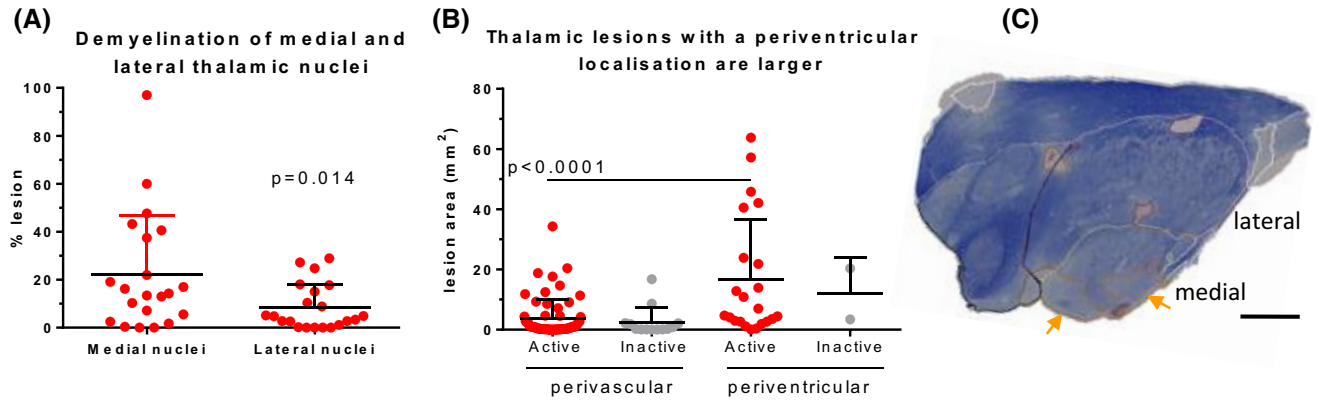

FIGURE 2 Regional vulnerability to inflammation and demyelination in the PMS thalamus. (A) The extent of demyelination was greater as a proportion of the area of the medial thalamus than it was of the lateral thalamus. (B) To investigate the contribution of perivascular or periventricular lesions to overall thalamic demyelinating pathology, we re-classified lesions based on their location in relation to the periventricular wall of the 3rd ventricular (referred to as periventricular) or if the lesion was contained within the thalamus without contacting the ependyma (referred to as perivascular). Lesions categorised as periventricular were larger (lesion area in mm^2) but less frequent (each data point represents a single lesion) than those 'perivascular' lesions. (C) LFB-stained section of the thalamus from case MS497 with a large chronic active lesion located along the ependymal margins of the block (orange arrow and orange line annotation). Mann-Whitney or Wilcoxon paired test. Scale bar: D = 5 mm

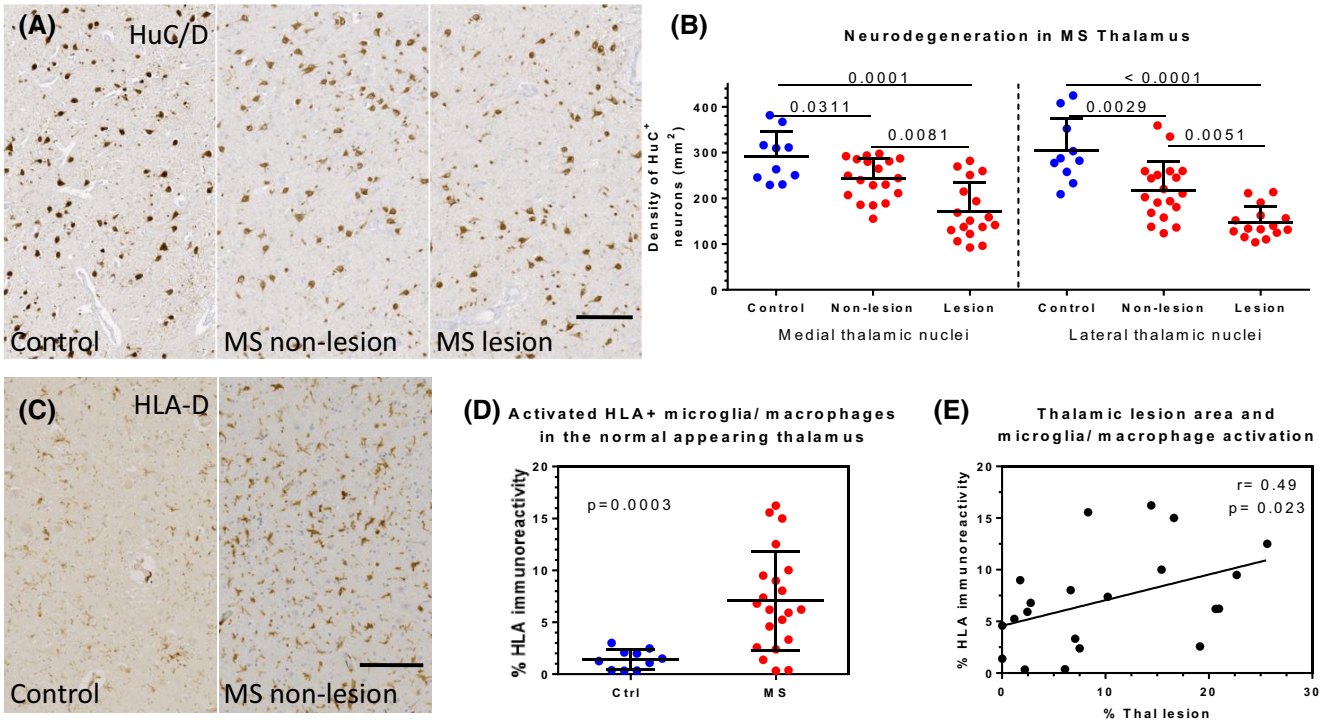

FIGURE 3 Significant neurodegeneration and widespread microglia/macrophage activation in the PMS thalamus. (A) Whole tissue sections immunostained with anti-HuC/D to reveal post-mitotic neurons in control, non-lesion and lesion medial thalamic nucleus. Quantification revealed a significant reduction in the density of HuC/D+ neurons per mm^2 in non-lesion and lesion medial and lateral thalamus (red data points) in comparison to region matched controls (blue data points). The non-lesion thalamus was characterised by an elevated area of anti-HLA-D immunoreactivity (C, D) in comparison to control tissue. The area of HLA-D immunoreactivity correlated modestly with the extent of thalamic demyelination in the same case (E). Kruskal-Wallis test with Dunn's multiple comparison post-test (B), Mann-Whitney test (D), Spearman's correlation (E). Ctrl, control. Scale bars: A, C = 100 μm

grey matter for the same cases: comparing normal thalamus neuron count (as a percentage of control) to cortical grey matter neuron count as a percentage of control (76.43 ± 15.33% vs 82 ± 17%, $p = 0.296$), and comparing total thalamus neuron count in lesion thalamus (compared to control) to lesion cortical grey matter neuron count (56.04 ± 15.31% vs 75.8 ± 21.5%, $p = 0.003$).

The density of HLA-D+ microglia/macrophages was elevated in non-lesion thalamus ($p < 0.0003$; Figure 3C,D). The area of HLA-D+ immunoreactivity did not correlate

with neuronal densities in non-lesion ($r = 0.36$, $p = 0.124$) or lesioned thalamus ($r = 0.48$, $p = 0.056$, Spearman correlation), but correlated modestly with the extent of total thalamic demyelination (Spearman $r = 0.49$, $p = 0.023$; Figure 3E).

3.5 | The extent of thalamic neurodegeneration correlated with forebrain white matter lesion load and a more severe disease outcome

To further understand the interplay between the local and distal pathologies on neuron loss in the PMS thalamus a correlative analysis was performed. An association was seen between the extent of neuronal loss in the normal MS thalamus (medial and lateral nuclei counts combined to generate an average per case) and the extent of forebrain white matter demyelination ($r = 0.79$, $p < 0.0001$), indicating that extra-thalamic pathological events are likely to be contributory to thalamic neurodegeneration (Figure 4A). This association between neuron loss and forebrain white matter demyelination was particularly strong when comparing neuron loss in the non-lesion lateral thalamic nuclei ($r = 0.80$, $p < 0.0001$) in comparison to the medial nuclei ($r = 0.55$, $p = 0.015$). A significant association was also seen between the extent of thalamic neuronal loss and disease duration (Figure 4B) and age of death (Figure 4C). The extent of thalamic demyelination is modestly associated with disease duration but not with the age of death or forebrain white matter demyelination (Figure 4D–F). The extent of thalamic anti-HLA-D+ immunoreactivity did not associate with forebrain pathology or disease outcome measures (Figure 4G–I). The extent of neuron loss in the forebrain cortical grey matter (averaged across frontal, cingulate and temporal lobe grey matter) or the extent of sub-cortical white matter demyelination in the same samples, did not associate with disease duration or age of death (Spearman $r = 0$ to -0.3, $p > 0.05$; data not shown).

3.6 | Complement is synthesised and activated local to actively demyelinate thalamic lesions

Robust parenchymal and membrane-associated immunostaining of the complement recognition molecule C1q, and the products of early complement activation, C4d, Bb and C3b, were seen in MS thalamus (Figure 5). Complement C1q is principally generated by activated microglia and we noted robust C1q protein at the expanding chronic active lesion edge. (Figure 5A–C) and also deposited on neurons (Figure 5D). Complement C3b was found in astrocytes, where it distinguishes a population of reactive and damaging glia and within, and upon, occasional neurons (Figure 5F–H). All components of the complement system can be generated in the CNS [56]. *In situ* hybridisation confirmed local *C1QA* and *C3* synthesis in the non-lesion PMS thalamus, where transcripts were seen associated with neurons (anti-HuC/D+ positive) and non-neuronal cells (Figure 5E,I,J). Immunoreactivity for C4d and Bb was detected on neurons, glia and more diffusely in the parenchyma (Figure 5K,L). We did not see extensive evidence of complement activation to completion: anti-MAC immunoreactivity was infrequent and essentially restricted to abluminal aspects of the vasculature and the choroid epithelium, e.g. (Figure 5M, arrows). Anti-complement C1q, C4d, C3b, Bb and MAC immunoreactivity was seen in all samples of thalamus prepared from four cases of acute viral encephalitis (Figure S1, Table 1). Anti-MAC immunoreactivity was seen along the vasculature and parenchyma at sites of focal microglial/macrophage activation in these same tissues. C3b immunoreactive neurons and glia close to disrupted vessels, areas of diffuse parenchymal immunoreactivity near the vasculature and labelling of the glial limitans were seen in the cases of acute and chronic ischaemic encephalopathy (supplementary 1). C1q and C3b staining of cells and neuropil were less evident in non-neurological controls (Figure 5N,O), with immune reactivity mostly confined to the vasculaure and glial limiting membrane. C1-inhibitor immunolabelling was noted on cells and the vasculature in both control and MS thalamus (Figure 5P,Q).

A significant increase in anti-complement C1q immunoreactivity was observed in normal-appearing thalamus in comparison to matched non-neurological controls (Figure 6A, $p = 0.008$), which was mirrored by a significant increase in anti-C4d immunoreactivity (Figure 6B, $p = 0.011$). Anti-C1q and anti-C4d immunoreactivity was elevated in the active and CAD lesions in comparison to the non-lesion thalamus (Figure 6A,B; $p < 0.05$). Anti-C1q and -C4d immunoreactivity in chronic inactive lesions were unchanged from levels seen in the non-lesioned thalamus or the control thalamus. Anti-C3b quantitative immunohistochemistry revealed a similar extent of increased immunoreactivity at sites of inflammatory demyelination as seen for anti-C1q and -C4d (Figure 6C). The relative area of C1q immunoreactivity is associated with the area of C3b immunostaining (Spearman $r = 0.47$, $p = 0.047$). Fragment Bb, a product of activation of the alternative complement pathway, was significantly elevated in CAD lesions in comparison to normal-appearing thalamus (Figure 6D; $p = 0.001$).

Anti-C1-inhibitor immunoreactivity was unchanged, or reduced in extent, in comparison to control tissue in the same ROIs assessed for complement activation, including at the CAD lesion edge, where anti-C1q and -C4d immunoreactivity were increased (Figure 6E). These data suggest a dysregulation of complement at the level of classical pathway activation. Of interest, we noted that the relative area of C1q immunoreactivity per case inversely correlated with the area of anti-C1-inhibitor signal (Spearman correlation of per cent area

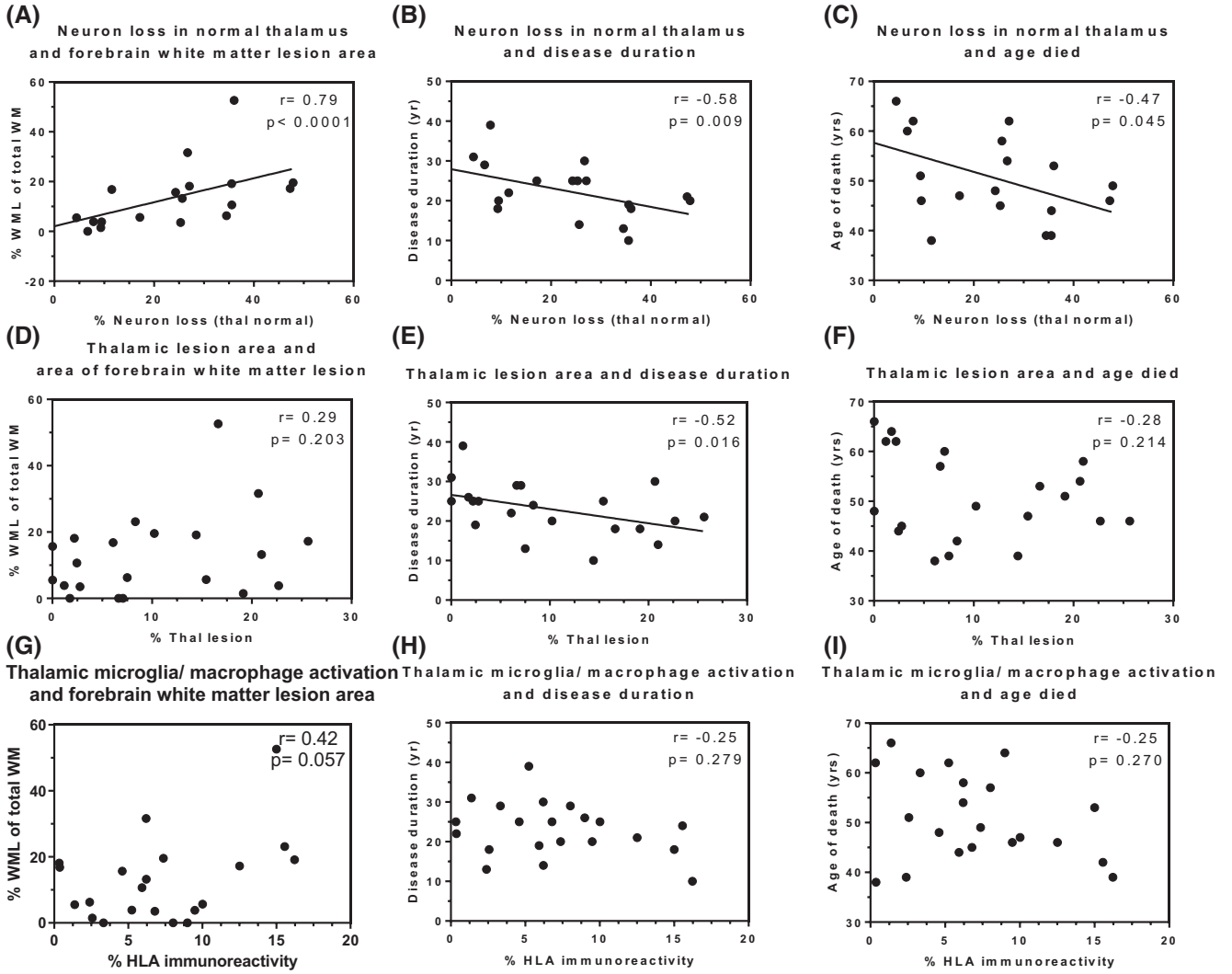

FIGURE 4 Neuron loss in the non-lesion thalamus associated with wider brain pathology and clinical disease outcome. By comparing the per cent neuron loss in the normal thalamus (A–C; % neuron loss thal normal), the relative area of thalamic demyelination (D–F; % Thal lesion) or the extent of HLA-D+ immunoreactivity (G–I; % HLA immunoreactivity), we show that it is the extent of neuronal loss in the normal-appearing thalamus that most closely associated with the extent of forebrain white matter lesion load (A; of total measured forebrain white matter), disease duration (B) and age of death (C). Spearman's correlation analysis comparing data means for each case (represented as a single data point) with Spearman r- and p-values shown. WML, white matter lesion

C1q immunoreactivity in the non-lesion thalamus with per cent area C1-inhibitor immunoreactivity, $r = -0.670$, $p = 0.002$). We did not see any significant associations between the relative area of complement immunoreactivity and neuron density in the lesion or non-lesion thalamus. Only a trend ($p = 0.05$–0.077) was seen between the area of C3b immunostain and neuron loss, HLA-D+ area or lesion size (Figure 6F; Spearman r- and p-values for each comparison shown).

4 | DISCUSSION

Here, we report that the thalamus in post-mortem progressive MS is characterised pathologically by extensive active inflammatory demyelination, neuronal loss, activation of complement and microglia. Thalamic lesions were larger and more frequent in medial nuclei and those bordering the subependymal space were the largest lesion type described. Conversely, neuronal loss was greatest in the lateral nuclei and associated with the extent of forebrain white matter demyelination, suggesting an important role for antero/retrograde degenerative processes. The extent of thalamic neurodegeneration correlated with shorter disease duration and a younger age at death. Local increases in complement activation may play an important role in sustaining long-standing active inflammatory demyelination and neurodegeneration, which are associated with a more severe clinical outcome.

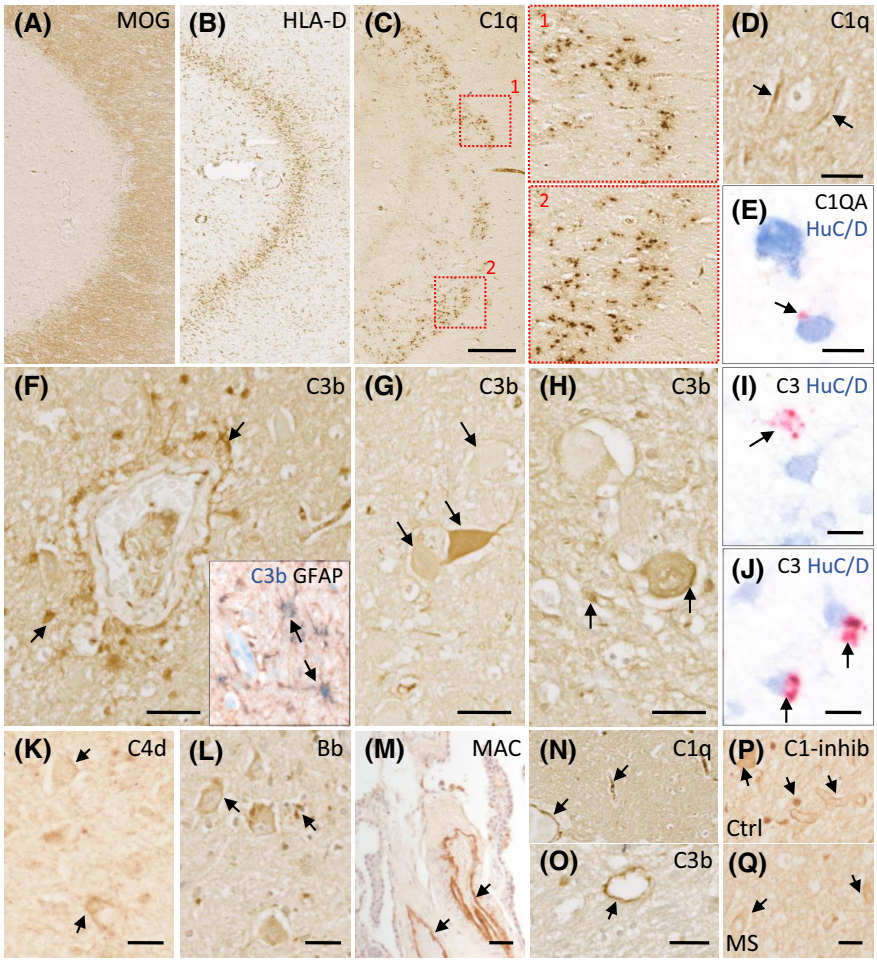

FIGURE 5 Local complement synthesis and activation in the PMS thalamus. (A–C) Representative images of anti-C1q, immunostaining at a chronic active demyelinating lesion edge. (D) Alongside a co-distribution with areas of microglial activation, anti-C1q immunostaining was also noted at discreet peri-neuronal sites (arrows). (E) Evidence of local complement C1QA synthesis (*C1QA* transcript revealed by the fast red chromogen abutting a HuC/D+ neuron (arrow)). (F) C3b was noted at perivascular sites and upon/within GFAP positive astrocytes (inset, arrows showing GFAP- brown and C3b- blue, co-labelling revealed by sequential double immunohistochemistry). (G–J) Evidence of both non-neuronal and neuronal anti-C3b immunoreactivity (G, H) and C3 transcript (arrows in I and J, identifying C3 transcript (fast Red chromogen, arrows) in sections immunostained with anti-HuC/D antisera). (K, L) Anti-C4d and Bb immunostained cells of the thalamus. MAC (C5b-9) was essentially restricted to the brain connective tissue spaces, such as the choroid epithelium of the inferior blade of the lateral ventricle (M, arrows). (N, O) C1q and C3b immunostaining of non-diseased control thalamus mainly decorated the vasculature. (P, Q) Examples of anti-C1-inhibitor immunostained cells and vasculature of the medial thalamus in control and MS (arrows). MAC, membrane attack complex. Scale bars: A–C = 100 μm; D–L, P, Q = 20 μm; M–O = 50 μm

4.1 | The thalamus is characterised by an active demyelinating pathology

Deep grey matter structures of the basal ganglia and thalamus are widely affected at all stages of MS. Their increased susceptibility to damage is likely to be the consequence of a number of factors, including: their proximity to the inflammatory milieu of the CSF; the thalamus being highly vascularised and within watershed areas of the brain; the thalamus being rich in iron that can enhance oxidative injury upon release from damaged and dying cells [15,57],the presence of their extensive functional connections [58]. These conditions make the thalamus particularly vulnerable to antero/retrograde inflammatory and degenerative pathologies. Such susceptibility makes the assessment of thalamic volume, and decreasing volume over time, an appealing and potentially sensitive indicator of disease severity, including accrued disability and cognitive dysfunction [11,59–61]. Our analysis of coronal samples of mid thalamus, using digital pathology approaches, reveals the thalamic nuclei to be substantially affected by an active inflammatory and demyelinating pathology relative to other grey matter areas examined.

The majority of thalamic lesions were characterised as active demyelinating or chronic active and were present in similar proportions to those in the sub-cortical white matter. The majority of cortical grey matter lesions in our cohort were characterised as chronic inactive lesions as is typical for progressive MS [62]. As radiological monitoring of chronic active/slowly expanding lesions is described as a useful indicator of clinical progression

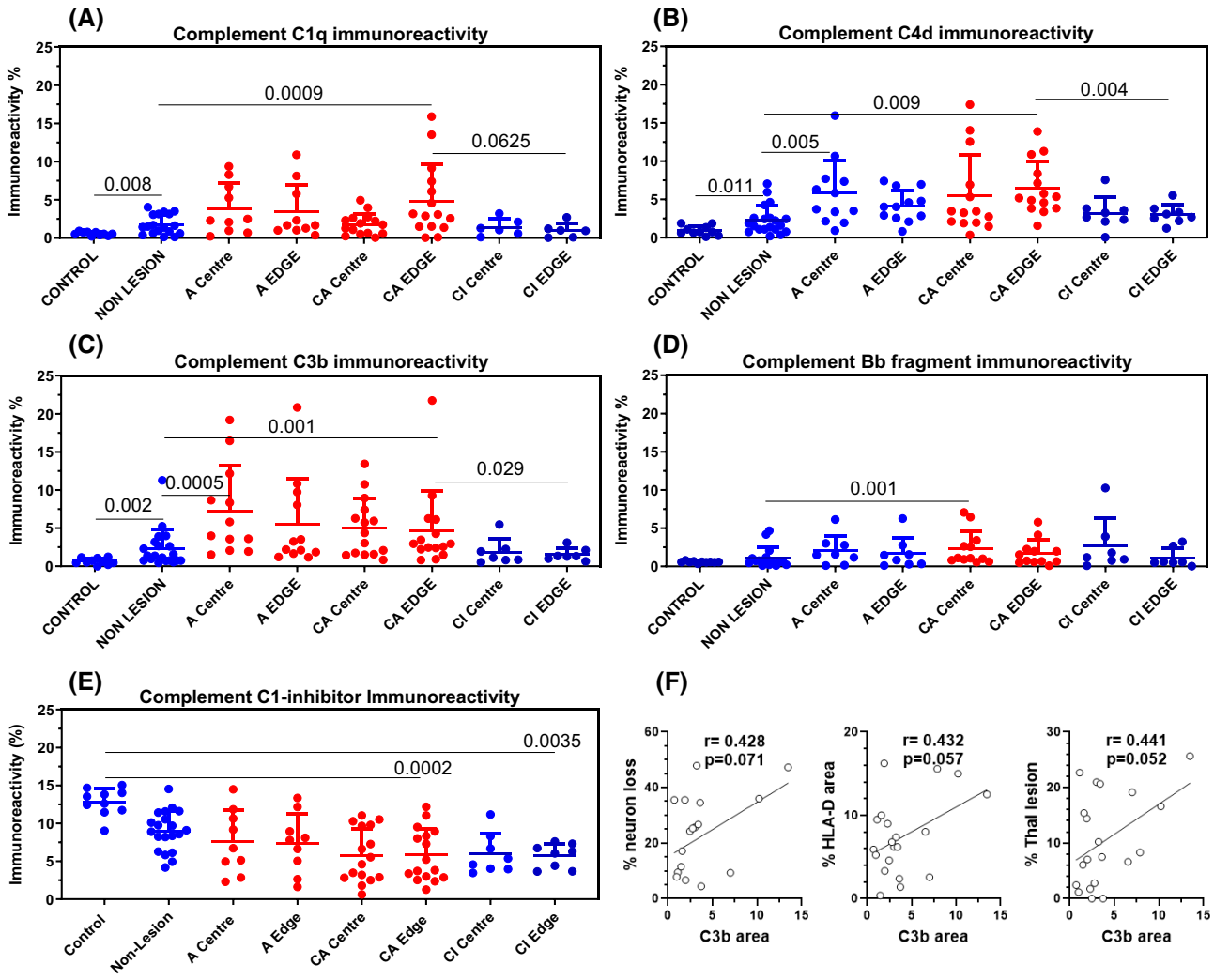

FIGURE 6 Complement activation and dysregulation in the PMS thalamus. Quantification of the area of immunoreactivity of anti-C1q (A), anti-C4d (B), anti-C3b (C) and anti-Bb (D) in control, non-lesion and lesion areas (lesion centre and edge of active, chronic active and demyelinating and chronic inactive lesions) revealed significant complement immunoreactivity at areas of active inflammatory demyelinating pathology in comparison to control or non-lesion tissue. Complement classical pathway C1q and C4d were additionally elevated in the normal-appearing (non-lesion) PMS thalamus in comparison to control. In the same regions of interest, expression of the complement regulatory protein, C1-inhibitor, was unchanged or significantly decreased (E) in comparison to the control thalamus. (F) Only a trend to an association was noted between the area of C3b immunoreactivity and wider measures of thalamic pathology (Spearman correlation analysis and Spearman r and p values shown). A centre, A edge, active lesion centre or edge sample; CA, chronic active; CI, chronic inactive. Kruskal-Wallis multiple comparison test with Dunn's post-test

[63,64], our finding that the number of cases presenting with active thalamic lesions was greater than the number of cases presenting with active white matter lesions, suggests that identifying such chronic active lesions in the thalamus would be invaluable for recognising those PMS cases with an active disease who might respond to current immunomodulatory therapies [65,66].

Alongside widespread active inflammatory demyelinating lesions, we noted a significant increase in the density of HLA-D+ activated microglia/macrophages in normal-appearing, non-lesioned thalamus. Positron emission tomography targeting TSPO identifies areas of elevated microglial density in the human brain [67,68]. Increased radioligand uptake reflecting greater TSPO+ cell density in the thalamus is seen at all disease stages and is particularly evident in the progressive phase [69]. Increased signal uptake in the thalamus correlates with worsening disability status, timed 25-foot walk and a decreasing whole brain volume, for example. Such clinical studies serve to illustrate the value of quantifying thalamic microglial/macrophage density to assess disease severity [68].

The extent of demyelination was similar to that seen in sub-cortical white matter areas, but significantly less than seen across frontal, cingulate and temporal grey matter measured in the same cases. Factors that

contribute to the reduced extent of thalamic demyelination in comparison to the neocortex may include the larger pial surface-to-cortical area versus the less extensive ependymal surface-to-thalamus area, which would reduce exposure to pro-inflammatory CSF constituents. Additionally, the ependyma represents a more robust structural and immunological barrier, as it comprises fenestrated cells connected with tight junction assemblies, in contrast, the pia comprises fibroblast-like cells and simple squamous epithelium and lacks tight junctions [70,71]. In addition, the ependymal layer is an effective immunoregulatory barrier as it expresses an array of complement regulatory proteins, which may reduce the deleterious effects of pathogens, inflammatory cytokines and complement present in the CSF [33,72].

4.2 | Patterns of lesion distribution in the thalamus suggest relevant pathomechanisms of demyelination

The more extensive demyelination seen in the proximity of CSF-brain barriers, irrespective of anatomical location, is an important pathological feature of PMS and is most notable in cases with increased inflammatory infiltrates, enriched in B-cells and plasma cells, and an inflammatory CSF cytokine profile that is consistent with the presence of leptomeningeal inflammation [19,32,73–75]. In agreement with previous studies, our data shows significant areas of subependymal demyelination in the thalamus, which has also been seen in paediatric and adult-onset MS, whereby gradients of tissue injury, similar to those reported in the neocortex are apparent [76], and can be visualised with appropriate MRI procedures [16,77–80]. It should be noted that the extent of demyelination represents a continuum and that others, notably [17], reported fewer, smaller, and less active inflammatory subependymal thalamic lesions in their large cohort with an older age of death. The presence of tissue gradients of damage, being greatest nearest the CSF-associated surfaces and affecting the periventricular white and deep grey matter structures, neocortex, cerebellum and spinal cord, taken together with CSF immune profiling [19,81], could help identify those individuals with different dominant pathological drivers, who might benefit from therapies that deplete B-cells and other effector cell populations enriched in the CNS [82-84].

4.3 | Neurodegeneration in the thalamus correlated with disease severity

Extensive neurodegeneration characterises the MS thalamus [14,17,85]. We show that neuronal loss was greater in the non-lesioned lateral nuclei in comparison to the medial thalamus, implying that antero- and/or retrograde degeneration because of axonal interruption and/or neuronal cell death in the forebrain, may contribute to thalamic neurodegeneration [86]. Our findings are supported by recent imaging and pathological studies that reported thalamic tissue volume loss was more closely related to the extent of wider forebrain pathology than to thalamic lesion load itself [11,12,17,80]. These data further emphasise the combined pathogenic drivers affecting the thalamus, be they associated with the CSF-constituents of the ventricular system or connected structures of the distal white and grey matter.

4.4 | Local mediators of thalamic pathology: A role for complement in sustaining ongoing tissue destruction

Microglia/macrophages are an important source of complement and are themselves modulated by complement through their panel of receptors for surface-bound (e.g. C4d, C3b) and soluble (e.g. C3a and C5a) complement fragments. Complement is widely expressed in the chronic MS brain; levels of transcripts and protein are increased in lesion and non-lesion samples, and the density of C5a receptor-positive microglia/macrophages is elevated [30,31,34,37,38,49,87]. Complement gene networks are amongst those most enriched in human grey matter microglia [88], whilst a population of microglia, with C1q as a critical mediator of activation, has been described at the edge of expanding chronic active lesions [40]. These data suggest an important role for the complement, and its interactions with microglia/macrophages, in determining the outcome of chronic neuroinflammation.

Complement gene networks, with complement C3 as the hub, are differentially affected in multiple sclerosis. Gene pathway analysis has revealed that multiple single nucleotide polymorphisms in complement *C1QA*, complement receptor *CR1* and *C3* associate with pathological and clinical measures of MS severity [41], whilst a common polymorphism in *C3*, linked to increased C3 activity, is associated with greater grey matter atrophy and cognitive decline [89]. Individuals with more than four paramagnetic rim enhancing lesions carry significantly more complement risk variants than those with fewer such lesions [40]. Extensive experimental and neuropathological observations have shown a key role for complement C1q and C3 in mediating synapse removal by microglial phagocytosis in normal development and pathological settings [28,90], including within the retina, thalamus and hippocampus [42-44].

We and others have noted complement within and upon different CNS cells. All cells of the CNS are capable of synthesising complement and complement C1q and products of C3 are found intracellularly, where they may support normal homeostasis [91,92]. C3 can be proteolytically cleaved to yield C3a and C3b by lysosomal cathepsin L and is noted in cells as a response to acute tissue injury, where

it partly accounts for the severity of tissue damage and maybe important to T cell function [93,94]. Intracellular products of C3 cleavage, including C3b and C3d, are a hallmark of a neurotoxic astrocyte, seen experimentally and at post-mortem [39]. Our findings of intracellular complement in neurons, which replicates the findings of others (e.g. [34,37,44]) may well be a consequence of non-specific uptake by some cells (for example, the intense C3b immunoreactive cells near vessels in ischaemic encephalopathy [supplementary] but were not seen in this same perivascular distribution in PMS), whilst complement gene transcription may be secondary to distal injury. Clearly, more work needs to be done to fully understand the role of complement, and products of complement activation, in neuron health and the setting of chronic neuroinflammation.

We and others have previously shown that alternative pathway regulation may be dysfunctional in MS and that classical pathway markers C1q and C4d are associated with the extent of neuroinflammation and astroglia dysfunction [39,40,47,49]. C1q and the C4 activation fragment, C4d, were elevated in actively demyelinating thalamic MS lesions, whilst at the same sites, C1-inhibitor immunoreactivity was reduced or unchanged, in comparison to normal-appearing or control thalamus (and negatively correlated with the extent of C1q immunostain). Anti-MAC immunoreactivity was only seen in the most active PMS cases and was restricted to the choroid epithelium and vasculature. Regulators of MAC formation, CD59 and clusterin, are produced intrathecally and at elevated levels in MS, which may explain this observation [33,38]. As a result of the redundancy that exists in the network of complement regulators, it would be interesting to investigate the expression of other regulatory proteins, particularly those targeting early complement processing, to better understand the nature of this dysfunctional response [95].

4.5 | Study limitations

All quantitative analysis was automated using QuPath to ensure that larger areas of total or demyelinated thalamus and cortical regions could be assessed microscopically to improve the robustness of our findings. Unlike neuronal quantification, the analysis of the area of anti-complement and anti-HLA-D immunoreactivity was restricted to representative ROIs, as we needed to understand the spatial expression at relevant sites of the lesion and non-lesion tissue. Although this did mean that our capacity to detect significant associations between immune activation, e.g. the extent of complement activation, and neuronal loss or demyelination, was compromised.

4.6 | Conclusions

Our results support the hypothesis that multiple pathological processes are at play in the PMS thalamus, which may account for its widespread inflammatory and active demyelinating pathology. The individual nuclei of the PMS thalamus may be differentially affected by a combination of retrograde and anterograde degeneration from white matter lesions and neurodegeneration, CSF-mediated damage and intrinsic inflammatory processes, including the chronic activation of complement, which is synthesised locally. Our data support imaging of the thalamus combined with fluid markers, including those of early complement activation such as C1q, C3b and C4d (whereby C1q has recently been shown to be a modifiable target in experimental models) [40], to monitor disease severity and response to therapy.

ACKNOWLEDGEMENTS

We would like to thank Dr Djordje Gveric and the team of the UK MS Society Tissue Bank (The Multiple Sclerosis Society Tissue Bank is funded by the Multiple Sclerosis Society of Great Britain and Northern Ireland [registered charity 207495]), and Drs Carolyn Sloan and Marie Hamard at the Oxford Brain Bank (supported by the Medical Research Council, Brains for Dementia Research, Alzheimer Society and Alzheimer Research UK, Autistica UK and the NIHR Oxford Biomedical Research Centre). BPM and RB are supported by the UK Dementia Research Institute Cardiff, funded by the MRC.

CONFLICT OF INTEREST

RM received grant funding support from the Italian MS Foundation and F. Hoffmann La Roche. RR received speaker honoraria and consulting fees from F. Hoffmann La Roche, Novartis and MedImmune and funding from the UK MS Society. OWH received consulting fees from F. Hoffmann La Roche, paid to his institute, and grant funding support from the UK MS Society and Life Science Research Network Wales.

AUTHOR CONTRIBUTIONS

BC, JN and OWH designed the study. BC, MD, RL, LW, BP, EG, and RB performed the experiments and collected data. BC, BPM, RR, RM, JN and OWH analysed and interpreted the data and wrote the manuscript. All authors read and approved the final version of the manuscript.

ETHICS APPROVAL

This study was performed under research ethical approval 13/WA/0292 and 08/MRE09/31.

DATA AVAILABILITY STATEMENT

Upon reasonable request to the corresponding author.

ORCID

Owain W. Howell https://orcid.org/0000-0003-2157-9157

REFERENCES

1. Reynolds R, Roncaroli F, Nicholas R, Radotra B, Gveric D, Howell O. The neuropathological basis of clinical progression in multiple sclerosis. Acta Neuropathol. 2011;122:155–70.
2. Filippi M, Rocca MA, Barkhof F, Brück W, Chen JT, Comi G, et al. Association between pathological and MRI findings in multiple sclerosis. Lancet Neurol. 2012;11:349–60.
3. Calabrese M, Romualdi C, Poretto V, Favaretto A, Morra A, Rinaldi F, et al. The changing clinical course of multiple sclerosis: a matter of gray matter. Ann Neurol. 2013;74:76–83.
4. Popescu V, Agosta F, Hulst HE, Sluimer IC, Knol DL, Sormani MP, et al. Brain atrophy and lesion load predict long term disability in multiple sclerosis. J Neurol Neurosurg Psychiatry. 2013;84:1082–91.
5. Eshaghi A, Prados F, Brownlee WJ, Altmann DR, Tur C, Cardoso MJ, et al. Deep gray matter volume loss drives disability worsening in multiple sclerosis. Ann Neurol. 2018;83:210–22.
6. Mesaros S, Rocca MA, Absinta M, Ghezzi A, Milani N, Moiola L, et al. Evidence of thalamic gray matter loss in pediatric multiple sclerosis. Neurology. 2008;70:1107–12.
7. Ramasamy DP, Benedict RHB, Cox JL, Fritz D, Abdelrahman N, Hussein S, et al. Extent of cerebellum, subcortical and cortical atrophy in patients with MS: a case-control study. J Neurol Sci. 2009;282:47–54.
8. Calabrese M, Rinaldi F, Mattisi I, Bernardi V, Favaretto A, Perini P, et al. The predictive value of gray matter atrophy in clinically isolated syndromes. Neurology. 2011;77:257–63.
9. Zivadinov R, Havrdová E, Bergsland N, Tyblova M, Hagemeier J, Seidl Z, et al. Thalamic atrophy is associated with development of clinically definite multiple sclerosis. Radiology. 2013;268:831–41.
10. Azevedo CJ, Cen SY, Khadka S, Liu S, Kornak J, Shi Y, et al. Thalamic atrophy in multiple sclerosis: A magnetic resonance imaging marker of neurodegeneration throughout disease. Ann Neurol. 2018;83:223–34.
11. Magon S, Tsagkas C, Gaetano L, Patel R, Naegelin Y, Amann M, et al. Volume loss in the deep gray matter and thalamic subnuclei: a longitudinal study on disability progression in multiple sclerosis. J Neurol. 2020;267:1536–46.
12. Bergsland N, Benedict RHB, Dwyer MG, Fuchs TA, Jakimovski D, Schweser F, et al. Thalamic nuclei volumes and their relationships to neuroperformance in multiple sclerosis: a cross-sectional structural MRI study. J Magn Reson Imaging. 2021;53:731–9.
13. Gilmore CP, Donaldson I, Bö L, Owens T, Lowe J, Evangelou N Regional variations in the extent and pattern of grey matter demyelination in multiple sclerosis: a comparison between the cerebral cortex, cerebellar cortex, deep grey matter nuclei and the spinal cord. J Neurol Neurosurg Psychiatry. 2009;80:182–7.
14. Vercellino M, Masera S, Lorenzatti M, Condello C, Merola A, Mattioda A, et al. Demyelination, inflammation, and neurodegeneration in multiple sclerosis deep gray matter. J Neuropathol Exp Neurol. 2009;68:489–502.
15. Haider L, Simeonidou C, Steinberger G, Hametner S, Grigoriadis N, Deretzi G, et al. Multiple sclerosis deep grey matter: the relation between demyelination, neurodegeneration, inflammation and iron. J Neurol Neurosurg Psychiatry. 2014;85:1386–95.
16. Louapre C, Govindarajan ST, Giannì C, Madigan N, Sloane JA, Treaba CA, et al. Heterogeneous pathological processes account for thalamic degeneration in multiple sclerosis: insights from 7 T imaging. Mult Scler J. 2018;24:1433–44.
17. Mahajan KR, Nakamura K, Cohen JA, Trapp BD, Ontaneda D Intrinsic and extrinsic mechanisms of thalamic pathology in multiple sclerosis. Ann Neurol. 2020;88:81–92.
18. Komori M, Blake A, Greenwood M, Lin YC, Kosa P, Ghazali D, et al. Cerebrospinal fluid markers reveal intrathecal inflammation in progressive multiple sclerosis. Ann Neurol. 2015;78:3–20.
19. Magliozzi R, Howell OW, Nicholas R, Cruciani C, Castellaro M, Romualdi C, et al. Inflammatory intrathecal profiles and cortical damage in multiple sclerosis. Ann Neurol. 2018;83:739–55.
20. Magliozzi R, Howell OW, Durrenberger P, Aricò E, James R, Cruciani C, et al. Meningeal inflammation changes the balance of TNF signalling in cortical grey matter in multiple sclerosis. J Neuroinflammation. 2019;16:259.
21. Spencer JI, Bell JS, DeLuca GC. Vascular pathology in multiple sclerosis: reframing pathogenesis around the blood-brain barrier. J Neurol Neurosurg Psychiatry. 2018;89:42–52.
22. Ingram G, Hakobyan S, Robertson NP, Morgan BP. Complement in multiple sclerosis: its role in disease and potential as a biomarker. Clin Exp Immunol. 2009;155:128–39.
23. Yates RL, Esiri MM, Palace J, Jacobs B, Perera R, DeLuca GC Fibrin(ogen) and neurodegeneration in the progressive multiple sclerosis cortex. Ann Neurol. 2017;82:259–70.
24. Magliozzi R, Hametner S, Facchiano F, Marastoni D, Rossi S, Castellaro M, et al. Iron homeostasis, complement, and coagulation cascade as CSF signature of cortical lesions in early multiple sclerosis. Ann Clin Transl Neurol. 2019a;6:2150–63.
25. Prineas JW, Kwon EE, Cho E-S, Sharer LR, Barnett MH, Oleszak EL, et al. Immunopathology of secondary-progressive multiple sclerosis. Ann Neurol. 2001;50:646–57.
26. Barnett MH, Prineas JW. Relapsing and remitting multiple sclerosis: pathology of the newly forming lesion. Ann Neurol. 2004;55:458–68.
27. Barnett MH, Parratt JDE, Cho E-S, Prineas JW. Immunoglobulins and complement in postmortem multiple sclerosis tissue. Ann Neurol. 2009;65:32–46.
28. Hong S, Beja-Glasser VF, Nfonoyim BM, Frouin A, Li S, Ramakrishnan S, et al. Complement and microglia mediate early synapse loss in Alzheimer mouse models. Science. 2016;352:712–6.
29. Sellebjerg F, Jaliashvili I, Christiansen M, Garred P. Intrathecal activation of the complement system and disability in multiple sclerosis. J Neurol Sci. 1998;157:168–74.
30. Ingram G, Loveless S, Howell OW, Hakobyan S, Dancey B, Harris CL, et al. Complement activation in multiple sclerosis plaques: an immunohistochemical analysis. Acta Neuropathol Commun. 2014;2:53.
31. Aeinehband S, Lindblom RPF, Al Nimer F, Vijayaraghavan S, Sandholm K, Khademi M, et al. Complement component C3 and butyrylcholinesterase activity are associated with neurodegeneration and clinical disability in multiple sclerosis. PLoS One. 2015;10:e0122048.
32. Bevan RJ, Evans R, Griffiths L, Watkins LM, Rees MI, Magliozzi R, et al. Meningeal inflammation and cortical demyelination in acute multiple sclerosis. Ann Neurol. 2018;84:829–42.
33. Zelek WM, Watkins LM, Howell OW, Evans R, Loveless S, Robertson NP, et al. Measurement of soluble CD59 in CSF in demyelinating disease: evidence for an intrathecal source of soluble CD59. Mult Scler. 2019;25:523–31.
34. Michailidou I, Naessens DMP, Hametner S, Guldenaar W, Kooi E-J, Geurts JJG, et al. Complement C3 on microglial clusters in multiple sclerosis occur in chronic but not acute disease: Implication for disease pathogenesis. Glia. 2017;65:264–77.
35. Storch MK, Piddlesden S, Haltia M, Iivanainen M, Morgan P, Lassmann H. Multiple sclerosis: in situ evidence for antibody- and complement-mediated demyelination. Ann Neurol. 1998;43:465–71.
36. Lucchinetti C, Brück W, Parisi J, Scheithauer B, Rodriguez M, Lassmann H. Heterogeneity of multiple sclerosis lesions: implications for the pathogenesis of demyelination. Ann Neurol. 2000;47:707–17.
37. Michailidou I, Willems JGP, Kooi E-J, van Eden C, Gold SM, Geurts JJG, et al. Complement C1q-C3-associated synaptic changes in multiple sclerosis hippocampus. Ann Neurol. 2015;77:1007–26.

38. Watkins LM, Neal JW, Loveless S, Michailidou I, Ramaglia V, Rees MI, et al. Complement is activated in progressive multiple sclerosis cortical grey matter lesions. J Neuroinflammation. 2016;13:161.
39. Liddelow SA, Guttenplan KA, Clarke LE, Bennett FC, Bohlen CJ, Schirmer L, et al. Neurotoxic reactive astrocytes are induced by activated microglia. Nature. 2017;541:481–7.
40. Absinta M, Maric D, Gharagozloo M, Garton T, Smith MD, Jin J, et al. A lymphocyte–microglia–astrocyte axis in chronic active multiple sclerosis. Nature. 2021;597:709–14.
41. Fitzgerald KC, Kim K, Smith MD, Aston SA, Fioravante N, Rothman AM, et al. Early complement genes are associated with visual system degeneration in multiple sclerosis. Brain. 2019;142:2722–36.
42. Werneburg S, Jung J, Kunjamma RB, Ha SK, Luciano NJ, Willis CM, et al. Targeted complement inhibition at synapses prevents microglial synaptic engulfment and synapse loss in demyelinating disease. Immunity. 2020;52:167–182.e7.
43. Gharagozloo M, Smith MD, Jin J, Garton T, Taylor M, Chao A, et al. Complement component 3 from astrocytes mediates retinal ganglion cell loss during neuroinflammation. Acta Neuropathol. 2021;142:899–915.
44. Ramaglia V, Dubey M, Malpede MA, Petersen N, de Vries SI, Ahmed SM, et al. Complement-associated loss of CA2 inhibitory synapses in the demyelinated hippocampus impairs memory. Acta Neuropathol. 2021;142:643–67.
45. Harold D, Abraham R, Hollingworth P, Sims R, Gerrish A, Hamshere ML, et al. Genome-wide association study identifies variants at CLU and PICALM associated with Alzheimer's disease. Nat Genet. 2009;41:1088–93.
46. Lambert J-C, Heath S, Even G, Campion D, Sleegers K, Hiltunen M, et al. Genome-wide association study identifies variants at CLU and CR1 associated with Alzheimer's disease. Nat Genet. 2009;41:1094–9.
47. Ingram G, Hakobyan S, Hirst CL, Harris CL, Pickersgill TP, Cossburn MD, et al. Complement regulator factor H as a serum biomarker of multiple sclerosis disease state. Brain. 2010;133:1602–11.
48. Lindblom RPF, Aeinehband S, Strom M, Al Nimer F, Sandholm K, Khademi M, et al. Complement Receptor 2 is increased in cerebrospinal fluid of multiple sclerosis patients and regulates C3 function. Clin Immunol. 2016;67:89–95.
49. Loveless S, Neal JW, Howell OW, Harding KE, Sarkies P, Evans R, et al. Tissue microarray methodology identifies complement pathway activation and dysregulation in progressive multiple sclerosis. Brain Pathol. 2017;28:507–20.
50. Luchetti S, Fransen NL, van Eden CG, Ramaglia V, Mason M, Huitinga I. Progressive multiple sclerosis patients show substantial lesion activity that correlates with clinical disease severity and sex: a retrospective autopsy cohort analysis. Acta Neuropathol. 2018;135:511–28.
51. Lassmann H. Pathogenic mechanisms associated with different clinical courses of multiple sclerosis. Front Immunol. 2019;10:1–14.
52. Macchi G, Jones EG. Toward an agreement on terminology of nuclear and subnuclear divisions of the motor thalamus. J Neurosurg. 1997;86:77–92.
53. Ding S-L, Royall JJ, Sunkin SM, Ng L, Facer BAC, Lesnar P, et al. Comprehensive cellular-resolution atlas of the adult human brain. J Comp Neurol. 2016;524:3127–481.
54. Bankhead P, Loughrey MB, Fernández JA, Dombrowski Y, McArt DG, Dunne PD, et al. QuPath: open source software for digital pathology image analysis. Sci Rep. 2017;7:16878.
55. Kuhlmann T, Ludwin S, Prat A, Antel J, Brück W, Lassmann H. An updated histological classification system for multiple sclerosis lesions. Acta Neuropathol. 2016;133:13–24.
56. Veerhuis R, Nielsen HM, Tenner AJ. Complement in the brain. Mol Immunol. 2011;48:1592–603.
57. Hametner S, Wimmer I, Haider L, Pfeifenbring S, Brück W, Lassmann H. Iron and neurodegeneration in the multiple sclerosis brain. Ann Neurol. 2013;74:848–61.
58. Hwang K, Bertolero MA, Liu WB, D'Esposito M. The human thalamus is an integrative hub for functional brain networks. J Neurosci. 2017;37:5594–607.
59. Minagar A, Barnett MH, Benedict RHB, Pelletier D, Pirko I, Sahraian MA, et al. The thalamus and multiple sclerosis: Modern views on pathologic, imaging, and clinical aspects. Neurology. 2013;80:210–9.
60. Bisecco A, Rocca MA, Pagani E, Mancini L, Enzinger C, Gallo A, et al. Connectivity-based parcellation of the thalamus in multiple sclerosis and its implications for cognitive impairment: a multicenter study. Hum Brain Mapp. 2015;36:2809–25.
61. Kipp M, Wagenknecht N, Beyer C, Samer S, Wuerfel J, Nikoubashman O. Thalamus pathology in multiple sclerosis: from biology to clinical application. Cell Mol Life Sci. 2015;72:1127–47.
62. Kutzelnigg A, Lucchinetti CF, Stadelmann C, Brück W, Rauschka H, Bergmann M, et al. Cortical demyelination and diffuse white matter injury in multiple sclerosis. Brain. 2005;128:2705–12.
63. Absinta M, Sati P, Masuzzo F, Nair G, Sethi V, Kolb H, et al. Association of chronic active multiple sclerosis lesions with disability in vivo. JAMA Neurol. 2019;76:1474–83.
64. Elliott C, Belachew S, Wolinsky JS, Hauser SL, Kappos L, Barkhof F, et al. Chronic white matter lesion activity predicts clinical progression in primary progressive multiple sclerosis. Brain. 2019;142:2787–99.
65. Fox RJ. How common is active inflammation in progressive multiple sclerosis? Nat Rev Neurol. 2021;17:463–4.
66. Mathey G, Ancel T, Garot T, Soudant M, Pittion-Vouyovitch S, Guillemin F, et al. Clinical and radiological activity of secondary progressive multiple sclerosis in a population-based cohort. Eur J Neurol. 2021;28:2238–48.
67. Nutma E, Stephenson JA, Gorter RP, de Bruin J, Boucherie DM, Donat CK, et al. A quantitative neuropathological assessment of translocator protein expression in multiple sclerosis. Brain. 2019;142:3440–55.
68. Singhal T, O'Connor K, Dubey S, Pan H, Chu R, Hurwitz S, et al. Gray matter microglial activation in relapsing vs progressive MS: A [F-18]PBR06-PET study. Neurol Neuroimmunol NeuroInflamm. 2019;6:e587.
69. Herranz E, Giannì C, Louapre C, Treaba CA, Govindarajan ST, Ouellette R, et al. The neuroinflammatory component of gray matter pathology in multiple sclerosis. Ann Neurol. 2016;80:776–90.
70. Jiménez AJ, Domínguez-Pinos MD, Guerra MM, Fernández-Llebrez P, Pérez-Fígares JM. Structure and function of the ependymal barrier and diseases associated with ependyma disruption. Tissue Barriers. 2014;2:1–14.
71. Mastorakos P, McGavern D. The anatomy and immunology of vasculature in the central nervous system. Sci Immunol. 2019;4:1–15.
72. Canova C, Neal JW, Gasque P. Expression of innate immune complement regulators on brain epithelial cells during human bacterial meningitis. J Neuroinflammation. 2006;3:22.
73. Griffiths L, Reynolds R, Evans R, Bevan RJ, Rees MI, Gveric D, et al. Substantial subpial cortical demyelination in progressive multiple sclerosis: have we underestimated the extent of cortical pathology? Neuroimmunol Neuroinflamm. 2020;7:51–67.
74. Howell OW, Reeves CA, Nicholas R, Carassiti D, Radotra B, Gentleman SM, et al. Meningeal inflammation is widespread and linked to cortical pathology in multiple sclerosis. Brain. 2011;134:2755–71.
75. Reali C, Magliozzi R, Roncaroli F, Nicholas R, Howell OW, Reynolds R. B cell rich meningeal inflammation associates with increased spinal cord pathology in multiple sclerosis. Brain Pathol. 2020;30:779–93.

76. Magliozzi R, Howell OW, Reeves C, Roncaroli F, Nicholas R, Serafini B, et al. A Gradient of neuronal loss and meningeal inflammation in multiple sclerosis. Ann Neurol. 2010;68:477–93.
77. Mainero C, Louapre C, Govindarajan ST, Gianni C, Nielsen AS, Cohen-Adad J, et al. A gradient in cortical pathology in multiple sclerosis by in vivo quantitative 7 T imaging. Brain. 2015;138:932–45.
78. Brown JWL, Pardini M, Brownlee WJ, Fernando K, Samson RS, Prados Carrasco F, et al. An abnormal periventricular magnetization transfer ratio gradient occurs early in multiple sclerosis. Brain. 2017;140:387–98.
79. Fadda G, Brown RA, Magliozzi R, Aubert-Broche B, O'Mahony J, Shinohara RT, et al. A surface-in gradient of thalamic damage evolves in pediatric multiple sclerosis. Ann Neurol. 2019;85:340–51.
80. De Meo E, Storelli L, Moiola L, Ghezzi A, Veggiotti P, Filippi M, et al. In vivo gradients of thalamic damage in paediatric multiple sclerosis: a window into pathology. Brain. 2021;144:186–97.
81. Bajrami A, Magliozzi R, Pisani AI, Pizzini FB, Crescenzo F, Marastoni D, et al. Volume changes of thalamus, hippocampus and cerebellum are associated with specific CSF profile in MS. Mult Scler J. 2021;1–11.
82. Bhargava P, Kim S, Reyes AA, Grenningloh R, Boschert U, Absinta M, et al. Imaging meningeal inflammation in CNS autoimmunity identifies a therapeutic role for BTK inhibition. Brain. 2021;144:1396–408.
83. Schafflick D, Xu CA, Hartlehnert M, Cole M, Schulte-Mecklenbeck A, Lautwein T, et al. Integrated single cell analysis of blood and cerebrospinal fluid leukocytes in multiple sclerosis. Nat Commun. 2020;11:1–14.
84. Johansson D, Rauld C, Roux J, Regairaz C, Galli E, Callegari I, et al. Mass Cytometry of CSF Identifies an MS-Associated B-cell Population. Neurol Neuroimmunol Neuroinflamm. 2021;8:1–10.
85. Cifelli A, Arridge M, Jezzard P, Esiri MM, Palace J, Matthews PM. Thalamic neurodegeneration in multiple sclerosis. Ann Neurol. 2002;52:650–3.
86. Kolasinski J, Stagg CJ, Chance SA, Deluca GC, Esiri MM, Chang EH, et al. A combined post-mortem magnetic resonance imaging and quantitative histological study of multiple sclerosis pathology. Brain. 2012;135:2938–51.
87. Ramaglia V, Hughes TR, Donev RM, Ruseva MM, Wu X, Huitinga I, et al. C3-dependent mechanism of microglial priming relevant to multiple sclerosis. Proc Natl Acad Sci U S A. 2012;109:965–70.
88. van der Poel M, Ulas T, Mizee MR, Hsiao CC, Miedema SSM, Adelia, et al. Transcriptional profiling of human microglia reveals grey–white matter heterogeneity and multiple sclerosis-associated changes. Nat Commun. 2019;10:1139.
89. Roostaei T, Sadaghiani S, Mashhadi R, Falahatian M, Mohamadi E, Javadian N, et al. Convergent effects of a functional C3 variant on brain atrophy, demyelination, and cognitive impairment in multiple sclerosis. Mult Scler J. 2019;25:532–40.
90. Schafer DP, Lehrman EK, Kautzman AG, Koyama R, Mardinly AR, Yamasaki R, et al. Microglia sculpt postnatal neural circuits in an activity and complement-dependent manner. Neuron. 2012;74:691–705.
91. Ricklin D, Reis ES, Mastellos DC, Gros P, Lambris JD. Complement component C3 – The "Swiss Army Knife" of innate immunity and host defense. Immunol Rev. 2016;274:33–58.
92. Reichhardt MP, Meri S. Intracellular complement activation—An alarm raising mechanism? Semin Immunol. 2018;38:54–62.
93. Liszewski MK, Kolev M, Le Friec G, Leung M, Bertram PG, Fara AF, et al. Intracellular complement activation sustains T cell homeostasis and mediates effector differentiation. Immunity. 2013;39:1143–57.
94. Satyam A, Kannan L, Matsumoto N, Geha M, Lapchak PH, Bosse R, et al. Intracellular activation of complement 3 is responsible for intestinal tissue damage during mesenteric ischemia. J Immunol. 2017;198:788–97.
95. Merle NS, Church SE, Fremeaux-Bacchi V, Roumenina LT. Complement system part I—molecular mechanisms of activation and regulation. Front Immunol. 2015;6:262.

SUPPORTING INFORMATION

Additional supporting information may be found in the online version of the article at the publisher's website.

FIGURE S1 Complement and microglial activation in neuroinflammatory and hypoxic-ischaemic disease controls. Coronal samples of thalamus from cases of viral encephalitis (A–H; see Table 1) displayed both focal and diffuse activated microglia (A, B). Classical pathway components C1q, C4d and the regulator C1-inhibitor, were expressed along the vasculature, parenchyma and soma (C–E). Anti-complement C3b and fragment Bb immunostaining was evident in all cases (F, G). Terminal complement pathway activation was evidenced by the presence of discreet parenchymal anti-MAC immunoreactivity in all samples analysed. (I–K) Anti-C3b immunostaining of three cases of acute or chronic ischaemic encephalopathy. Note the intense labelling of perivascular cells in I (and inset in boxed panel), staining of the glial limitans and patches of diffuse C3b immunostainof the parenchyma (J, K, arrows). Scale bars: A, B = 10 μm; C-L = 25 μm

How to cite this article: Cooze BJ, Dickerson M, Loganathan R, Watkins LM, Grounds E, Pearson BR, et al. The association between neurodegeneration and local complement activation in the thalamus to progressive multiple sclerosis outcome. Brain Pathol. 2022;32:e13054. https://doi.org/10.1111/bpa.13054